Mechanism of chirality conversion by periodic change of temperature: Role of chiral clusters

Hiroyasu Katsuno[1,*] and Makio Uwaha[2,†]
[1]*Department of Physical Science, Ritsumeikan University, 1-1-1 Noji-higashi, Kusatsu 525-8577, Japan*
[2]*Department of Physics, Nagoya University, Furo-cho, Chikusa-ku, Nagoya 464-8602, Japan*
(Received 29 August 2015; published 11 January 2016)

By grinding crystals in a solution, the chirality of crystal structure (and the molecular chirality for the case of chiral molecules as well) can be converted, and the cause of the phenomenon is attributed to crystal growth with chiral clusters. We show that the recently found chirality conversion with a periodic change of temperature can also be explained by crystal growth with chiral clusters. With the use of a generalized Becker-Döring model, which includes enantio-selective incorporation of small chiral clusters to large solid clusters, the change of cluster distribution and the mass flow between clusters are studied. The chiral clusters act as a reservoir to pump out the minority species to the majority, and the exponential amplification of the enantiomeric excess found in the experiment is reproduced in the numerical calculation.

DOI: 10.1103/PhysRevE.93.013002

I. INTRODUCTION

Several years after Viedma's discovery of chirality conversion of $NaClO_3$ crystals by grinding in a solution [1], Noorduin *et al.* successfully applied the grinding method to organic crystals, where the chirality conversion of crystals simultaneously implies conversion of the molecular chirality [2]. In these experiments, the crystal enantiomeric excess (CEE: relative excess of one of the crystal chiral species) grows exponentially in time [1–12], although some exceptions have been found [11,13]. Steendam *et al.* attributed the exceptional linear behavior to the existence of impurities [11]. The common exponential behavior suggests that a nonlinear autocatalytic process is involved.

In order to find the mechanism of chirality conversion, several theoretical models have been proposed. Uwaha [14,15] used reaction-equation-type models by assuming a steady distribution of crystal sizes and showed the exponential growth of CEE. The essential idea of the model is that chiral growth units (small chiral clusters) contribute to the growth of crystals of the same chirality [16]. Grinding helps to produce such chiral clusters and keeps the steady size distribution. The assumption of a steady size distribution was confirmed [17] with the use of a generalized Becker-Döring (BD) model (classical nucleation model) [18]. Dissociation into monomers and nonlinear effect due to the cluster incorporation to crystals correspond to Saito and Hyuga's general conditions for realizing homochirality [19]. The time-evolution of cluster size distribution was studied from different view points [20–24] and all proved the role of chiral clusters to provide the exponential amplification of CEE.

Several other mechanisms have been proposed. One of the famous mechanisms in chiral symmetry breaking is a mutual inhibition. Its specific case by a geometrical shadowing effect in crystal growth [25–27] can be a cause of autocatalysis. Catalytic conversion of molecular chirality at the crystalline surface [28] is also the candidate. These models that reproduce the exponential increase of CEE are based on the idea of competition between nonlinearly growing chiral modes. The idea goes back to the Frank model [29], and has been applied to the experiment of spontaneous chiral symmetry breaking in $NaClO_3$ crystallization [30,31]. (See Refs. [32,33] for subsequent generalization of Franks idea.) Ostwald ripening is an important factor [34], but it is not capable of producing autocatalytic evolution [17,35,36]. Fluctuation of the system may also play a role, but it cannot give the exponential amplification and is effective only in very small systems [35–38].

Despite that experimental identification of the key mechanism is very difficult, ingenious experiments have revealed several features that may be significant to the chirality conversion. For a system of chiral molecules that racemize in a solution, Noorduin *et al.* indirectly showed that the enantiomeric excess in the solution is opposite to that in the solids [39]. The experiment supports enantioselective incorporation of clusters although other models are not totally excluded. Hein *et al.* [8] reported that during the period of the exponential amplification of CEE the size distribution of powder crystals becomes wider than that in other period of the grinding experiment. It was also noted that the initiation time of the exponential amplification is very diverse in this system. The authors suggested that an incidental formation and preservation of large crystals instigates the accelerated chirality conversion. It is not clear whether the change of the size distribution is a necessary condition for the chirality conversion because a steady size distribution is maintained during the amplification period in the generalized BD model [17]. Using $NaBrO_3$, Viedma *et al.* demonstrated that even macroscopic crystals of the same chirality may coagulate and form a large crystal [40]. It is also not clear how large clusters (or crystals) can coalesce to form a larger single crystal in real systems.

In the meanwhile, new experiments that show the exponential behavior without grinding appeared. Inspired by the experiment of El-Hachemi *et al.* [40], which showed a chiral symmetry breaking in the $NaClO_3$ crystallization in a boiling solution, Viedma and Cintas [41] found that a homochiral solid phase can be realized by simply boiling a solution containing

*katsuno@fc.ritsumei.ac.jp
†uwaha@nagoya-u.jp

 ©2016 American Physical Society

a racemic mixture of crystals [42]. The complexity of the experimental system hindered developing a theoretical model to study mechanism of the amazing phenomenon. Recently, Suwannasang *et al.* have performed a controlled experiment using an organic substance [43], and showed that periodic change of temperature of a solution with racemic powder crystals produces a homochiral state of crystals. Characteristic features of the experiment are: (1) the system was kept uniform by gentle stirring without grinding, (2) an exponential increase in CEE similar to that in Viedma ripening was observed, (3) the rate of the exponential increase was not sensitive to the period of the temperature cycle, and the increase almost stopped during a long period of constant temperature. It is a challenge for all existing physical models to explain the chirality conversion by the periodic change of temperature.

The purpose of the present paper is to study the possibility that the mechanism of enantioselective incorporation of clusters into chiral crystals can reproduce the chirality conversion without grinding and the above experimental features.

II. MODELS FOR CLUSTER GROWTH

In this section we briefly review several proposed models for chirality conversion. Most models that can reproduce the exponential autocatalytic behavior relies on nonlinear processes like enantioselective incorporation of chiral clusters (or agglomeration of chiral crystals) [14,15,17,20–24,35,36], catalytic conversion of molecular chirality at the surface [28], geometrical mutual inhibition [25–27] if models are correctly interpreted [44]. Since we are interested in the role of chiral clusters in the present paper, we restrict ourselves to the first ones.

The simple reaction-equation-type models [11,14,15,37,39] are easy to treat and interpret. Mathematically, a product term of the masses of chiral clusters and crystals, which represents incorporation of chiral clusters to solids of the same chirality, is the source of nonlinearity. The incorporation of chiral clusters accelerates the growth of major chirality and results in the exponential amplification of CEE. The simple models use only five or six components (monomers, chiral clusters, chiral solids), and the relative size distribution of crystals is assumed to be steady thanks to grinding [17]. Since intense grinding is necessary to keep the distribution steady, the reaction-equation-type models cannot be used for explaining the process of periodic change of temperature, in which the crystal size distribution changes with temperature (and time).

To study the size distribution of crystals, two different mean-field approaches have been adopted. One is generalization of the BD model (classical nucleation model), which takes account of the detailed balance condition for elementary processes to guarantee correct equilibrium states [17,18,21,23,45]. The other is generalization of a population-balance (PB) model, which is more versatile and commonly used in chemical engineering [22,24,46]. Taking the continuum limit of the BD equation, one obtains a Fokker-Plank equation, which has a drift term and a diffusion term in the size space [47]. The PB model corresponds to the Fokker-Planck equation without the diffusion term that is essential to study nucleation phenomena [18,48]. The PB model is useful when (macroscopic) breakage and agglomeration of crystals are important. For the use of such models care should be taken to use physically acceptable form of the terms in the PB equation. In any case, these models reproduce the exponential behavior, and at the moment we do not know the relevant size of clusters in real systems.

Another approach to study the size distribution is to follow the size change of each cluster using Monte Carlo (MC) dynamics [35,36]. These models can take the effect of fluctuations into account and demonstrated the role of fluctuation and that of clusters successfully. To obtain good statistics with changing conditions, however, the computational load is extremely heavy. MC lattice models developed by Saito and Huga [26–28] automatically include the cluster growth but have the same computational problem. Also separating the effect of cluster growth seems not easy in the lattice models. Therefore, in the present paper, we adopt the generalized BD model to study the possibility of chirality conversion by the periodic change of temperature.

III. GENERALIZED BECKER-DÖRING MODEL

The model we use in the present paper is a generalization of our previous model for Viedma ripening [17,18,45]. The following features are added to the standard BD model: (1) Monomers and clusters are distinguished by molecular chirality, and monomers can be transformed to the opposite chirality molecules. (2) Not only monomers but also small clusters up to a certain size, $j_{\max}$-mers, can be incorporated to large clusters of the same chirality. The rates of incorporation and dissociation satisfy the detailed balance condition. The following reactions of clusters are considered:

$$\begin{aligned} \mathrm{R}_1 &\rightleftharpoons \mathrm{L}_1, \quad \mathrm{R}_i + \mathrm{R}_j \rightleftharpoons \mathrm{R}_{i+j}, \\ \mathrm{L}_i + \mathrm{L}_j &\rightleftharpoons \mathrm{L}_{i+j}, \quad (\text{for } 1 \leqslant j \leqslant j_{\max}), \end{aligned} \tag{1}$$

where R_i and L_i represent an i-mer of the right-handed and left-handed molecule, respectively [49]. The reaction in the first line is spontaneous and at a constant probability for a molecule. The reactions to the right in the second line are proportional to the collision rate, and those to the left are such that they produce the canonical equilibrium distribution.

Thus we divide the molecules and the clusters into six groups according to their chirality and the size (monomers, small clusters, and large clusters). We will derive, in Sec. V, the mass flow between these groups during low- and high-temperature periods. The result is schematically depicted in Fig. 1. As explained in Sec. V, accelerated crystallization of the majority clusters causes surplus of the minority monomers, which leads to the chirality conversion from the minority to the majority species. The detail of the generalized BD model is as follows.

The number of right (R) or left (L)-handed (denoted as $\alpha = \mathrm{R}$ or L) large clusters of size i ($> j_{\max}$) obeys the equation

$$\begin{aligned} \dot{n}_i^\alpha = &\sum_{j=1}^{\min\{j_{\max},[(i+1)/2]\}} \sigma_{i-j,j} n_{i-j}^\alpha n_j^\alpha - \sum_{j=1}^{j_{\max}} \sigma_{i,j} n_i^\alpha n_j^\alpha \\ &+ \sum_{j=1}^{j_{\max}} \lambda_{i+j,j} n_{i+j}^\alpha - \sum_{j=1}^{\min\{j_{\max},[(i+1)/2]\}} \lambda_{i,j} n_i^\alpha, \end{aligned} \tag{2}$$

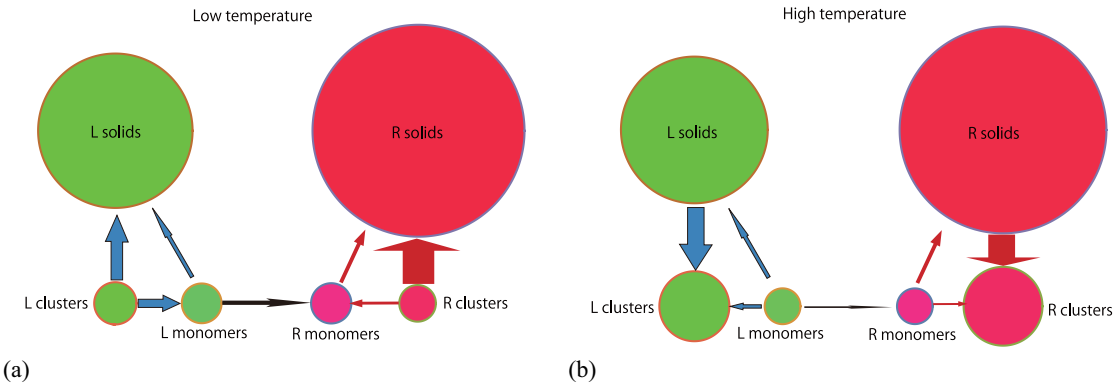

FIG. 1. Schematic mass flow at (a) low and (b) high temperatures.

where $[\cdots]$ in the upper limit of the summation is the floor function. The coefficient $\sigma_{i,j}$ represents the collision and coalescence of an i-mer and a j-mer, and is proportional to the collision cross-section. It is determined by the molecular cross sections and assumed to have the form

$$\sigma_{i,j} = a\, i^{2/3} j^{2/3}, \tag{3}$$

where a is a constant proportional to the thermal velocity and the cross section of a monomer. The decay rate $\lambda_{i+j,j}$ of an $(i+j)$-mer to an i-mer and a j-mer is determined from the detailed balance condition

$$\lambda_{i+j,j}\, n_{i+j}^{\alpha\,\mathrm{eq}} = \sigma_{i,j}\, n_i^{\alpha\,\mathrm{eq}}\, n_j^{\alpha\,\mathrm{eq}}, \tag{4}$$

where $n_i^{\alpha\,\mathrm{eq}}$ is the equilibrium number of (chiral) i-mers. Note that $n_i^{\mathrm{R\,eq}} = n_i^{\mathrm{L\,eq}} \equiv n_i^{\mathrm{eq}}$ with racemization. The equilibrium number of i-mers is related to that of monomers as

$$n_i^{\alpha\,\mathrm{eq}} = n_1^{\mathrm{eq}} e^{-\bar{\alpha}(i^{2/3}-1)}, \tag{5}$$

where $\bar{\alpha} = (4\pi)^{1/3}\Omega^{2/3}\alpha/k_{\mathrm{B}}T$ is an effective surface tension (Ω: molecular volume, α: surface tension). Therefore, we have

$$\lambda_{i+j,j} = \sigma_{i,j}\, n_1^{\mathrm{eq}} e^{\bar{\alpha}((i+j)^{2/3}-i^{2/3}-j^{2/3}+1)}. \tag{6}$$

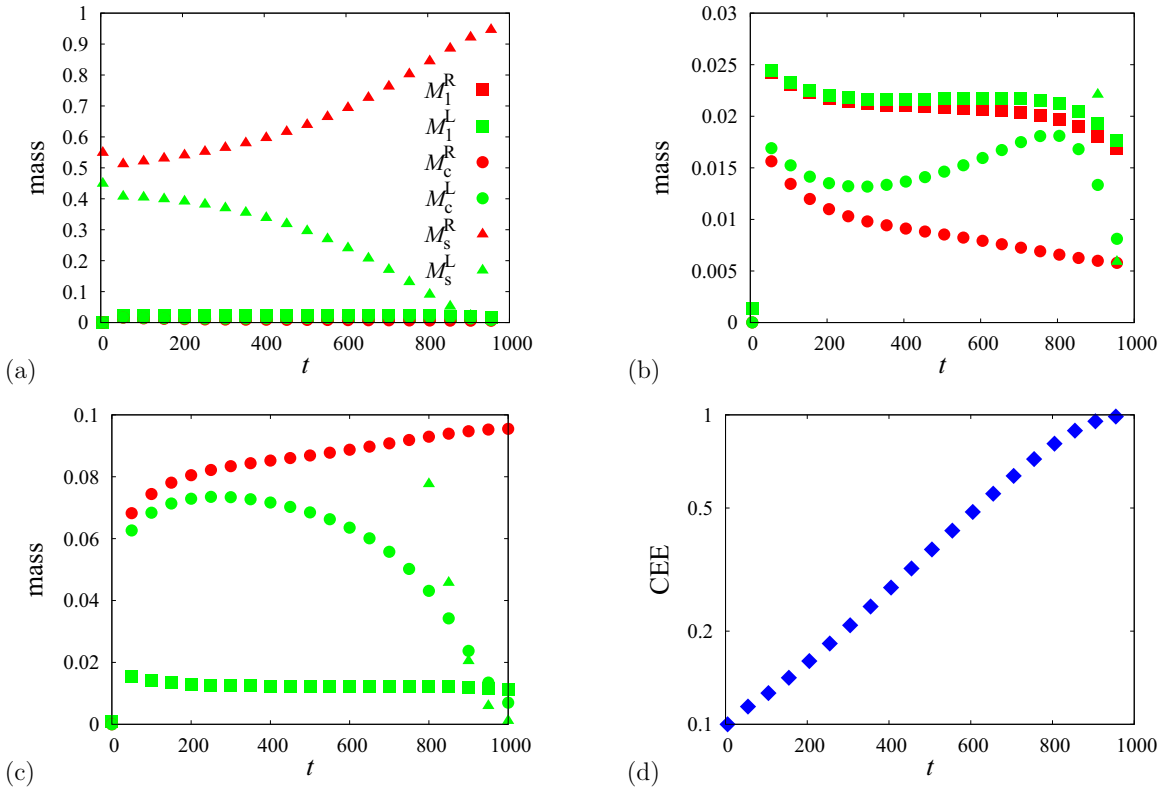

FIG. 2. (a) Change of masses of monomers, clusters, and solids by temperature cycling in the generalized BD model with $\phi(0) = 0.1$ at $t = (l + \frac{1}{2})P$. (b) Enlargement of the small mass part. (c) Enlargement at $t = lP$. Red (dark) squares are hidden by green (light) squares. (d) Semilog plot of CEE calculated from Eq. (10).

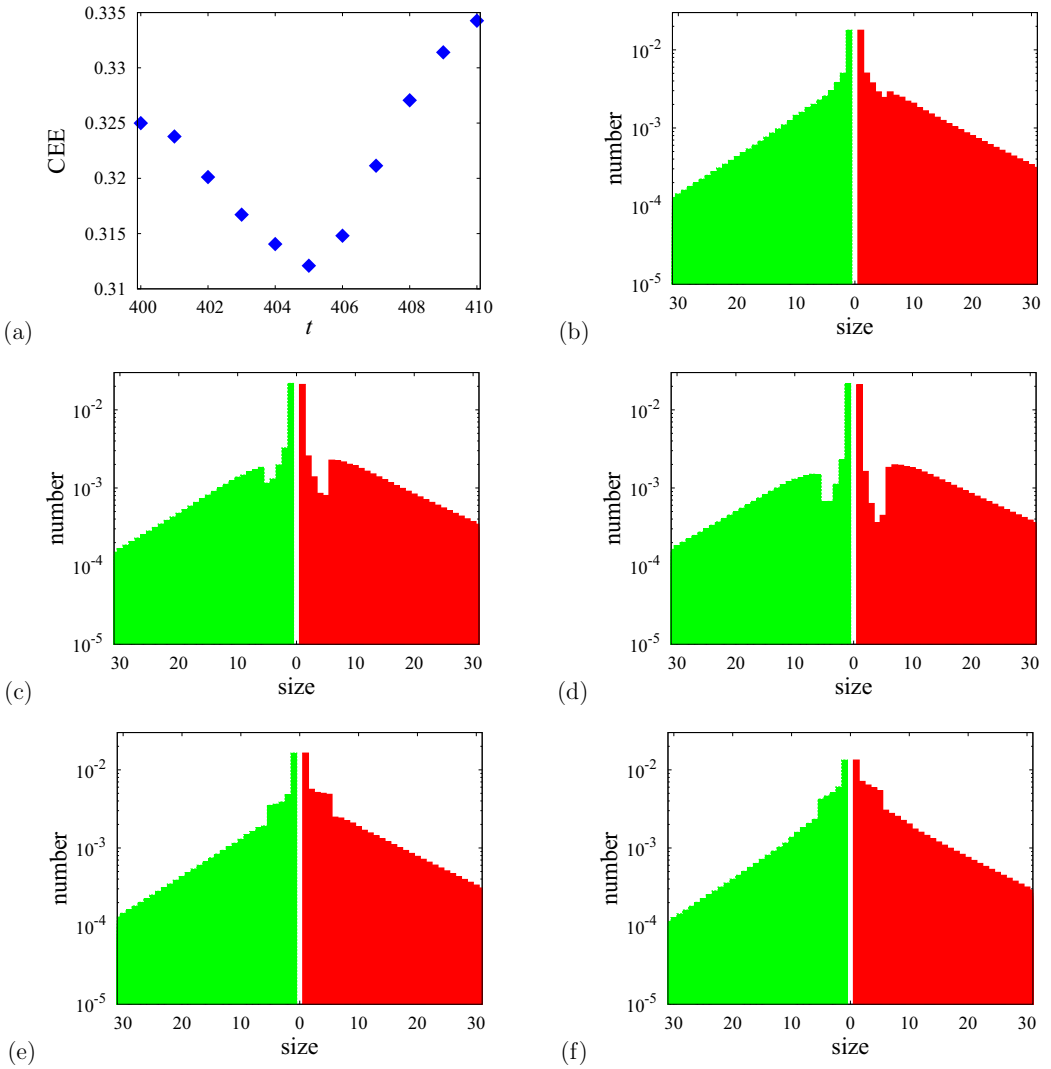

FIG. 3. (a) Change of CEE in the period $400 \leqslant t \leqslant 410$ (40th cycle). Size distribution of clusters at (b) $t = 401$, (c) $t = 403$, (d) $t = 405$, (e) $t = 407$, (f) $t = 409$. The right side and the left side on abscissa represent cluster size of R and L, respectively.

For small clusters, $2 \leqslant i \leqslant j_{\max}$, incorporation to any clusters is possible, and Eq. (2) is modified to

$$\dot{n}_i^\alpha = \sum_{j=1}^{[(i+1)/2]} \sigma_{i-j,j} n_{i-j}^\alpha n_j^\alpha - \sum_{j=1}^{\infty} (\sigma_{i,j} + \delta_{i,j}\sigma_{i,i}) n_i^\alpha n_j^\alpha + \sum_{j=1}^{\infty} (\lambda_{i+j,j} + \delta_{i,j}\lambda_{2i,i}) n_{i+j}^\alpha - \sum_{j=1}^{[(i+1)/2]} \lambda_{i,j} n_i^\alpha. \quad (7)$$

For monomers, $i = 1$, Eq. (7) applies with the additional racemization term

$$\dot{n}_1^{\mathrm{R,L}} = -2\sigma_{1,1}\left(n_1^{\mathrm{R,L}}\right)^2 - \sum_{j=2}^{\infty} \sigma_{1,j} n_1^{\mathrm{R,L}} n_j^{\mathrm{R,L}} + 2\lambda_{2,1} n_2^{\mathrm{R,L}} + \sum_{j=2}^{\infty} \lambda_{j+1,j} n_{j+1}^{\mathrm{R,L}} + r\left(n_1^{\mathrm{L,R}} - n_1^{\mathrm{R,L}}\right). \quad (8)$$

Note that our system in the present paper satisfies the detailed balance condition and there is no process, such as grinding, that breaks the detailed balance.

From now on we call clusters of the size $2 \leqslant i \leqslant j_{\max}$ small clusters or simply clusters, and clusters of the size $j_{\max} < i$ large clusters or solids. Then the masses of monomers, clusters, and solids are defined by

$$M_1^\alpha = n_1^\alpha,$$
$$M_{\mathrm{c}}^\alpha = \sum_{j=2}^{j_{\max}} j\, n_j^\alpha,$$
$$M_{\mathrm{s}}^\alpha = \sum_{j=j_{\max}+1}^{\infty} j\, n_j^\alpha, \quad (9)$$

respectively. It should be remembered that the present nomenclature is only provisional. We define the order parameter of the system by

$$\phi = \frac{M_{\mathrm{s}}^{\mathrm{R}} - M_{\mathrm{s}}^{\mathrm{L}}}{M_{\mathrm{s}}^{\mathrm{R}} + M_{\mathrm{s}}^{\mathrm{L}}}. \quad (10)$$

In the present paper we assume that the majority species is always R, then the definition of CEE is also given by Eq. (10).

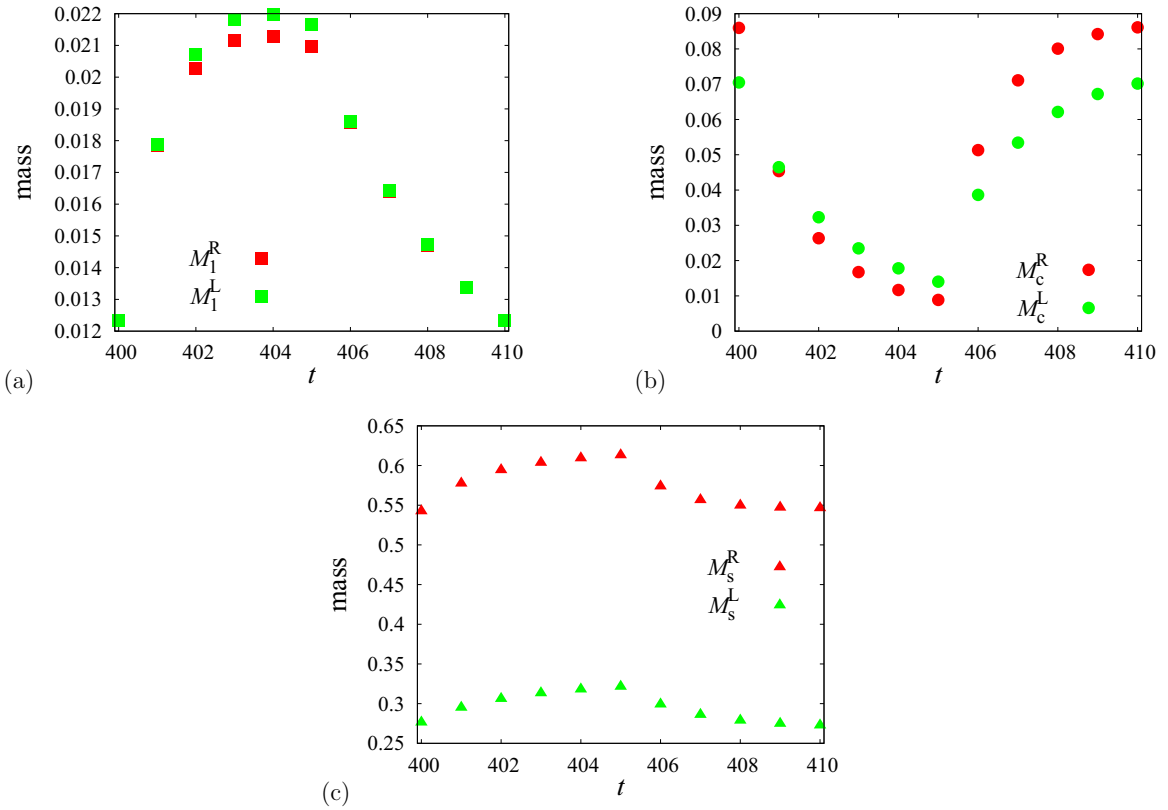

FIG. 4. Change of masses in one cycle: (a) R and L monomers, (b) R and L clusters, (c) R and L solids.

IV. NUMERICAL CALCULATION

A. Setup of numerical calculation

The basic setup of the numerical calculation is similar to our previous study of the chirality conversion with grinding [17], and the following features are added. We assume, for simplicity, that the change of temperature T is stepwise and cyclic with a period P:

$$T = T_{\rm l} \quad \text{for} \quad lP \leqslant t \leqslant \left(l+\frac{1}{2}\right)P,$$
$$T = T_{\rm h} \quad \text{for} \quad \left(l+\frac{1}{2}\right)P \leqslant t \leqslant (l+1)P, \qquad (11)$$

where the cycle number l is zero or a positive integer. We assume the incorporation rate $\sigma_{i,j}$ does not change and set $a = 1$ to fix the unit of time. Temperature-dependent physical parameters are the equilibrium monomer density $n_1^{\rm eq}$, the effective surface tension $\bar{\alpha}$, and the racemization rate r. In the present paper, the values for low and high temperatures are as follows: (1) $n_1^{\rm eq\,l} = 10^{-3}, n_1^{\rm eq\,h} = 10^{-2}$ (high solubility at high T), (2) $\bar{\alpha}^{\rm l} = 10, \bar{\alpha}^{\rm h} = 10^{-2}$ (low effective surface tension at high T), (3) $r^{\rm l} = 1, r^{\rm h} = 10$ (high racemization rate at high T). These values are chosen for easiness of the simulation and not necessarily correspondent to the real system.

The number of clusters is normalized to make the total mass (total number of molecules) unity

$$\sum_{\alpha}\sum_{i=1}^{\infty} i\, n_i^{\alpha} = 1, \qquad (12)$$

except in Sec. VI C. The initial system consists of racemic solid powder and the saturated solution. We have tried several different initial distributions, and have confirmed that the results are not too sensitive to the form of initial distributions. We adopt the following initial condition in most of our calculations:

$$n_i^{\rm R,L}(0) = n_i^{\rm eq\,l} + \delta_{i,i_{\rm s}} \frac{1 - 2\sum_{i=1}^{\infty} i\, n_i^{\rm eq\,l}}{i_{\rm s}} \frac{1 \pm \phi(0)}{2}, \qquad (13)$$

where the superscripts R and L correspond to the signs + and −, respectively: the initial system consists of large clusters of the size $i_{\rm s}$ with the initial CEE $\phi(0)$ and a racemic solution saturated at $T_{\rm l}$.

In the numerical calculation, the maximum cluster size of calculation is limited to $i_{\rm max}$, and the reaction which includes clusters larger than $i_{\rm max}$ is neglected: formation of clusters larger than $i_{\rm max}$ is forbidden. Since the number of clusters of this size in the most calculated time is so small, the resultant error is negligible. The maximum size is $i_{\rm max} = 200$ in the calculations of Sec. V, and $i_{\rm max} = 1000$ in the calculations of Sec. VI. With the above parameter values, the equilibrium mass in solution at $T_{\rm l}$ is $\sum_i i n_i^{\rm eq\,l} = 2.01 \times 10^{-3}$, and most of the molecules are initially in the solid clusters of $i = i_{\rm s}$. Values of other parameters are the period of cycle $P = 10$, the maximum size of solidifying small clusters $j_{\rm max} = 5$, and the initial size of the solid cluster $i_{\rm s} = i_{\rm max}$ unless mentioned otherwise.

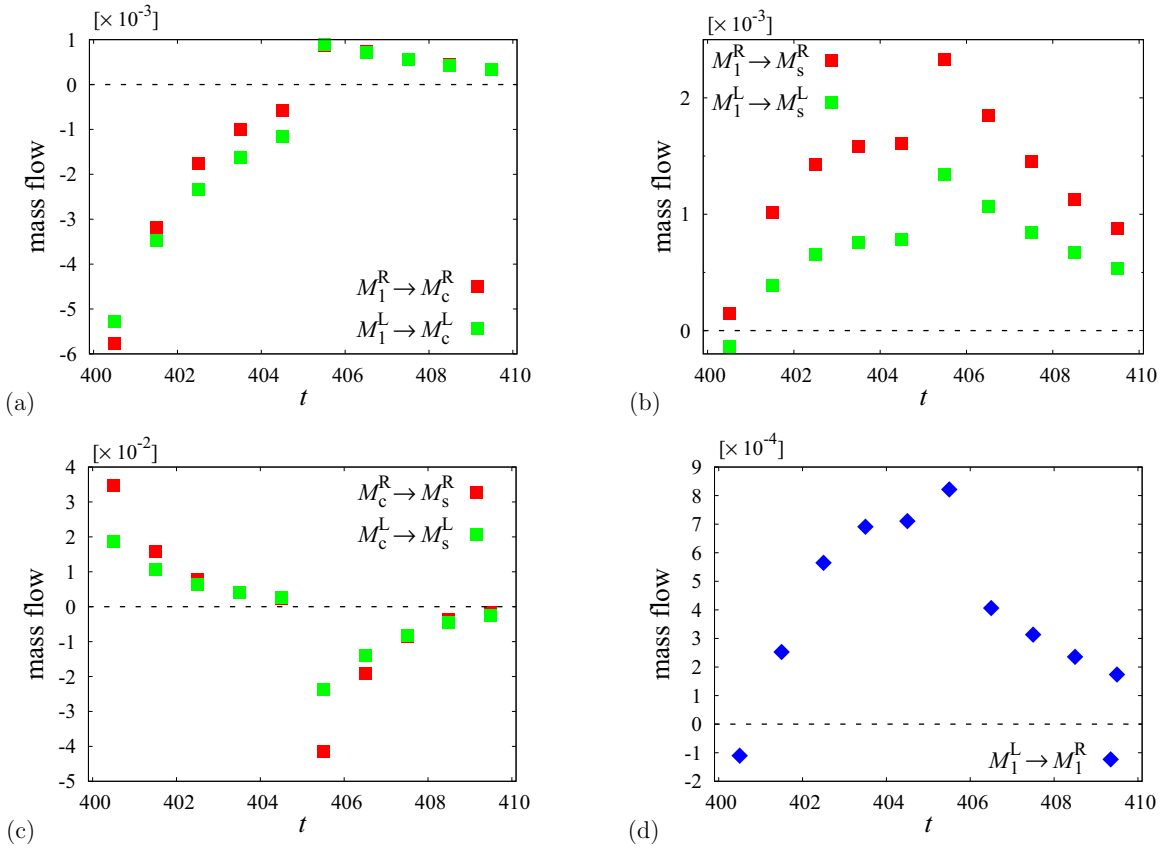

FIG. 5. Change of mass flow in one cycle: (a) from monomers to small clusters, (b) from monomers to solids, (c) from small clusters to solids, (d) from L monomers to R monomers.

B. Time change of the masses

Change of the masses calculated from a solution of the generalized BD Eqs. (2)–(8), are shown in Fig. 2 with the initial EE $\phi(0) = 0.1$. The mass of each component is monitored at the end of the low-temperature period in the cycle: $t = (l + \frac{1}{2})P$ [Figs. 2(a) and 2(b)], and at the end of the high temperature: $t = lP$ [Fig. 2(c)]. The masses of solids, M_s^R and M_s^L, show an exponential amplification of EE as shown in Fig. 2(d). The mass of the minority L monomers, M_1^L, is appreciably more than that of the majority R, M_1^R, during the strong amplification period. This is a necessary condition for conversion of chirality [15], and observed (though indirectly) in the experiment of chirality conversion with grinding [39]. The mass of L clusters, M_c^L, increases and much more than M_c^R during the amplification. At the end of the high-temperature period in the cycle $t = lP$, the mass of R monomers is almost the same as that of L, and the mass of R clusters is more than that of L [Fig. 2(c)]. Such features seem characteristic of chirality conversion by temperature cycling, and this is the important key to understand the mechanism as discussed in the following section.

V. ANALYSIS OF MASS FLOW AND THE ROLE OF CLUSTER GROWTH

By looking at the solution of the generalized BD model in more detail, we now study the role of cluster growth behind the scenes. In **A** we analyze the size distribution and mass flows between clusters during a typical temperature cycle in the period of exponential change of CEE and discuss the role of small clusters. In **B** the size of clusters relevant to the chirality conversion is identified.

A. Role of small clusters

In Fig. 3, the change of CEE and the size distribution in the 40th temperature cycle are plotted. The CEE decreases in the low-temperature period, $400 < t \leqslant 405$, and increases in the high-temperature period, $405 < t \leqslant 410$ [Fig. 3(a)]. The amount of the latter exceeds the former, and the CEE is amplified in one cycle. In Figs. 3(b)–3(f), the right side of the abscissa represents the cluster size of the majority type (R), and the left side represents that of the minority (L). The ordinate is the logarithm of the number of clusters. It is evident that the distribution of small clusters changes remarkably during the cycle: dips in the logarithmic plot at low temperatures and shoulders at high temperatures.

In order to see the change of each component more quantitatively, the masses of chiral monomers ($i = 1$), small clusters ($2 \leqslant i \leqslant 5$), and solids ($5 < i$) are plotted in Fig. 4, and to find the origin of the change, the mass flow between these components is shown in Fig. 5. The key feature of the chirality conversion is that the mass of the majority R clusters M_c^R is much more than M_c^L in the high-temperature period but less in the low-temperature period [Fig. 4(b)]. The mass flow between small clusters and solids is in accordance with our

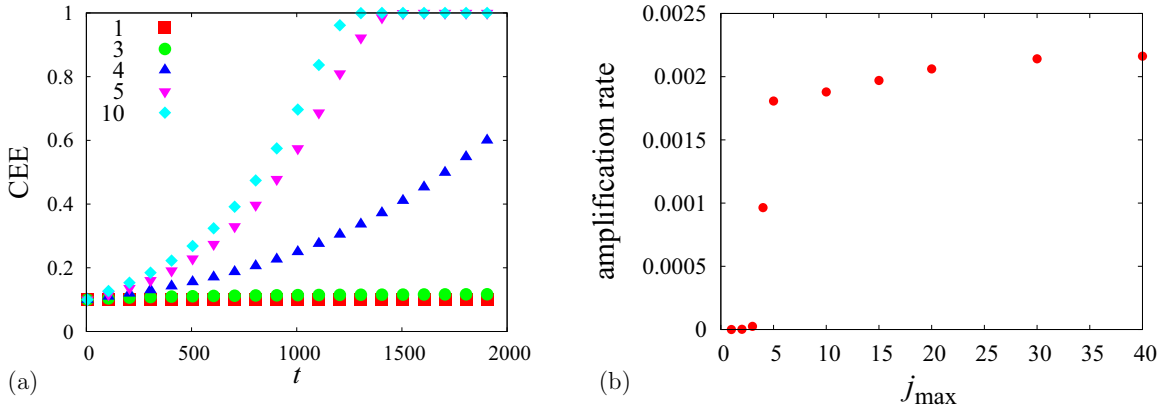

FIG. 6. (a) Change of CEE with various maximum size, j_{max}, of clusters that contribute to growth. (b) Amplification rate of CEE with various j_{max}.

common sense [Fig. 5(c)]: small clusters incorporate to large ones in the low-temperature period, and large ones melt to become small clusters in the high-temperature period. Since such mass flow with small clusters is much more effective than that of monomers [note that the magnitude in Fig. 5(c) is one order larger than in Figs. 5(a) and 5(b)], the behavior of small clusters controls the whole flow. In the beginning of low-temperature period, R clusters solidify twice as fast as L clusters [Fig. 5(c)], since R solid is twice as much as L solid [Fig. 4(c)]: the mass of R clusters decrease very rapidly to become less than M_c^L [Fig. 4(b)].

The mass flow from monomers to small clusters is positive in the high-temperature period and negative in the low-temperature period [Fig. 5(a)]. At the high temperature, monomers form small clusters because of the small effective surface tension [see Eq. (5)]. The mass of L monomers $M_1^L(=n_1^L)$ is appreciably higher than $M_1^R(=n_1^R)$ in most of the low-temperature period [Fig. 4(a)] because the fast solidification of R clusters leaves more L clusters, which dissociate to L monomers. Therefore, the chirality conversion at the molecular level from L to R takes place mainly in the low-temperature period [Fig. 5(d)] when the CEE decreases [Fig. 3(a)]. It is noteworthy that monomers are always supersaturated [Fig. 4(a)]: monomers of both chiralities increase in the low-temperature period high above the equilibrium value $n_1^{eq1} = 10^{-3}$, and decrease in the high-temperature period toward the equilibrium value, $n_1^{eqh} = 10^{-2}$. Then the mass flow from monomers to solids is positive for most of the temperature cycle [Fig. 5(b)]: monomers solidify even at the high temperature when solids melt into small clusters. Such excess of monomers at high temperature prohibits an increase in $n_1^R(M_1^R)$, which would have induced chirality conversion from R to L.

The whole process is depicted schematically in Fig. 1. In the low-temperature period, R clusters solidify much faster than L clusters since there are more R solids. Large numbers of R clusters are consumed by the solidification, and soon the mass of L clusters exceeds that of R ($M_c^L > M_c^R$). The clusters dissociate into monomers, resulting in the surplus of L monomers ($M_1^L > M_1^R$). The considerable excess of L monomers is maintained in most of the period, and it is the origin of the molecular chirality conversion. In the high-temperature period, rapid solid melting to small clusters takes place, and R clusters are formed more than L ($M_c^R > M_c^L$), while the number of monomers of both chiralities are roughly the same [Fig. 4(a)] because of the fast racemization. The increase of the CEE occurs in high-temperature melting, but the molecular chirality conversion takes place mainly in the low-temperature period.

B. Maximum size of clusters that contribute to growth

To find the size of clusters that promote the chirality conversion we performed numerical calculation with various values of j_{max}, which is the maximum size that contributes to growth. The change of CEE with various j_{max} is shown in Fig. 6(a), and the exponential amplification rates of these data are plotted in Fig. 6(b). The amplification rate ω is defined as

$$\phi(t) = \phi(0)e^{\omega t}, \tag{14}$$

and determined from the slopes in Fig. 6(a). Without cluster incorporation, $j_{max} = 1$, no change of CEE is seen. With $j_{max} = 2$ and 3, the very weak amplification occurs. In contrast, the amplification is remarkable with $j_{max} = 4$ and 5. The amplification rate ω increases with j_{max} but becomes saturated above $j_{max} = 5$. In the chirality conversion by grinding, the

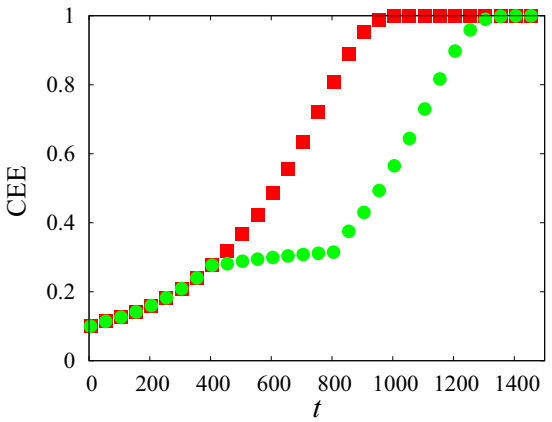

FIG. 7. Change of CEE with an interruption of temperature cycling in $400 < t < 800$.

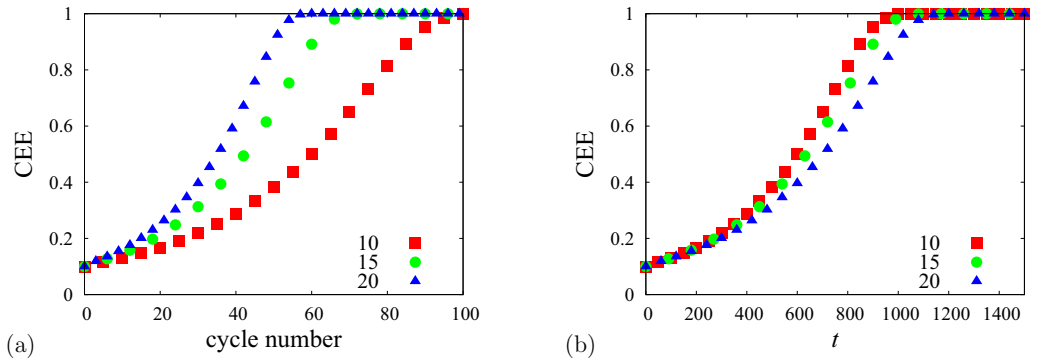

FIG. 8. Change of CEE for different periods of temperature cycling P. (a) as a function of cycles and (b) as a function of time.

exponential amplification of CEE is possible merely with the chiral dimer incorporation [17]. (The effect of larger clusters, $j_{\max} > 2$, is not studied in Ref. [17].) Without grinding, incorporation of larger clusters to solids seems necessary, but clusters larger than $j = 5$ do not accelerate the process much. Note that we have assumed the detailed balance condition Eq. (6).

VI. CHARACTERISTIC FEATURES IN THE EXPERIMENT

In the temperature cycling experiment [43] several interesting features were observed. In this section, we test whether our model can reproduce these experimental features.

A. Interruption of temperature cycling

In the experiment [43] the exponential amplification of CEE is suspended when the cycling is interrupted for a considerable duration. To test if our model shows such a behavior, the temperature cycling was interrupted in the period $400 < t < 800$. The result is shown in Fig. 7. The amplification is suspended during the interruption period. Only a very slow increase in the CEE is observed, which is in accordance with the experiment (Fig. 4 of Ref. [43]). Interruptions of other durations show similar behaviors.

B. Dependence on the period

Another feature of the experiment [43] is that the amplification rate of CEE is not sensitive to the period P. In Fig. 8 the changes of CEE for $P = 10, P = 20$, and $P = 30$ are shown. They roughly collapse to a single exponential curve as a function of time, whereas they show a large difference if plotted as a function of the cycle number. Figure 8 corresponds to the experimental result (Fig. 5 of Ref. [43]), although the temperature profiles are not identical and the comparison is only qualitative.

C. Dependence on the mass of crystals

When the total mass of crystals is increased in the experiment [43], the time necessary for complete conversion is increased accordingly. We performed several simulations with different mass of crystals by changing the initial amount of large clusters of the size i_s in Eq. (13), and the result is shown in Fig. 9(a) for the mass ratio 0.5, 1, 1.5, with $P = 25$. The mass ratio R is defined as the ratio of the initial solid mass to that in the previous numerical calculations. The amplification rate decreases when the mass is increased. As shown in Fig. 9(b), the time necessary for the complete chirality conversion is roughly proportional to the mass of crystals in accordance with the experiment (Fig. 6 in Ref. [43]).

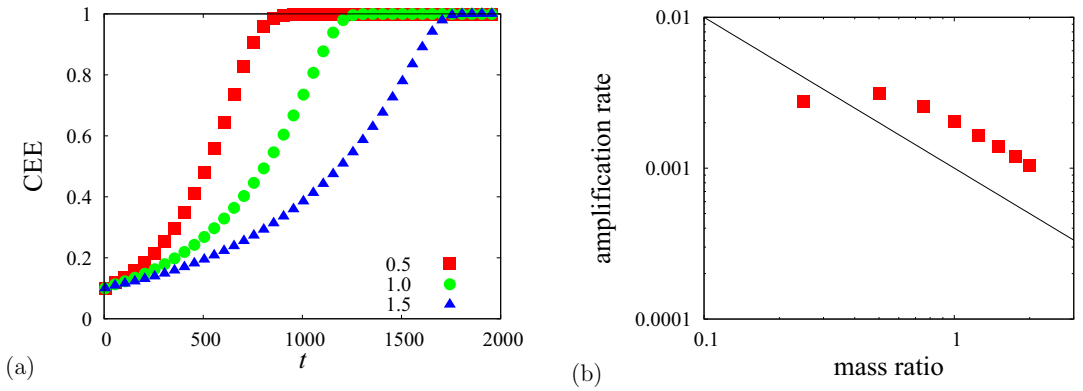

FIG. 9. (a) Change of CEE and (b) the amplification rate ω for different amounts of crystals. Mass ratio R is the amount of the initial solid mass to that in the previous calculation. In (b), the solid line represents R^{-1}.

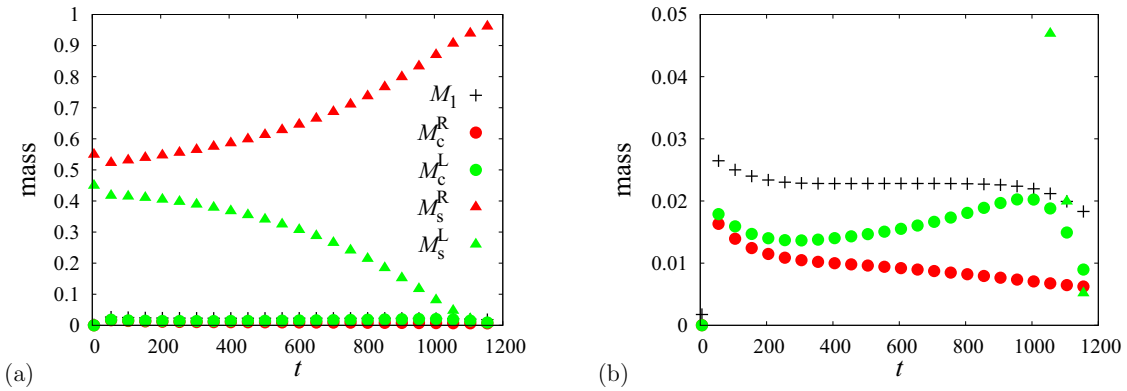

FIG. 10. (a) Change of masses of achiral monomers M_1, chiral clusters $M_c^{R,L}$, and chiral solids $M_s^{R,L}$ by temperature cycling with $\phi(0) = 0.1$ at $t = (l + \frac{1}{2})P$. (b) Enlargement of the small mass part.

VII. SYSTEM OF ACHIRAL MOLECULES

So far, we have studied the model system that corresponds to the experiment with chiral molecules [43]. Similar effects have been observed for the case of $NaClO_3$ [40,41]. Since systems of achiral molecules such as $NaClO_3$ and $NaBrO_3$ can be considered as systems of chiral molecules with extremely fast racemization, the same mechanism should work to realize nonlinear chirality conversion. We modify our model to have one type of achiral molecules and two types of small chiral clusters and chiral solid clusters, and the result is shown in Fig. 10. Masses of each component changes similarly to those in Fig. 2 as expected.

VIII. SUMMARY

The chirality conversion with the periodic change of temperature [43] can be explained by the same processes that explains Viedma ripening [14,17]: incorporation of small chiral clusters to solids of the same chirality and the dissociation of chiral clusters into monomers. We demonstrated the exponential amplification of an initial small CEE with the use of the generalized BD model [17,23], in which all elementary processes satisfy the detailed balance condition. The analysis in Sec. V shows that the small clusters work as a reservoir, which induces the chirality conversion. Solidification of the majority species is accelerated by the small clusters. The majority small clusters are consumed rapidly, and the minority small clusters, whose number soon exceeds the majority, dissociate into monomers (because of the large effective surface tension at low temperature) to produce more minority monomers. Then the surplus minority monomers are transformed into the majority monomers. As a whole, the temperature cycling transforms the minority species to the majority by using the chiral cluster state as a pump.

There are two theoretical explanations [23,50] relating the chirality amplification with temperature change. The first one considers mass exchange between high- and low-temperature systems, which may explain the experiment of steady circulation [41] but not the experiment of temperature cycling [43]. The second one [50] introduces an arbitrary assumption that the majority species crystallizes faster than the minority, which, we think, is not justifiable. Thus, the present scheme is the first reasonable explanation of the experiment with periodic change of temperature [43]. The choice of the parameter values adopted in the numerical calculation is rather arbitrary and sometimes a little extreme. The reason may be that the system size in the calculation is very limited. The maximum cluster size in the calculation is 10^3, and the simulation result should not be taken as quantitatively real but only as qualitative. It is important that both chirality conversions with grinding and with temperature cycling are explained by the same mechanism: incorporation of chiral clusters to solids and dissociation of clusters to monomers.

ACKNOWLEDGMENTS

The present research is supported by JSPS KAKENHI Grants No. 24540318 and No. 15K05127.

[1] C. Viedma, Phys. Rev. Lett. **94**, 065504 (2005).
[2] W. L. Noorduin, T. Izumi, A. Millemaggi, M. Leeman, H. Meekes, W. J. P. Van Enckevort, R. M. Kellogg, B. Kaptein, E. Vlieg, and D. G. Blackmond, J. Am. Chem. Soc. **130**, 1158 (2008).
[3] B. Kaptein, W. L. Noorduin, H. Meekes, W. J. P. van Enckevort, R. M. Kellogg, and E. Vlieg, Angew. Chem. Int. Ed. **47**, 7226 (2008).
[4] P. S. M. Cheung, J. Gagnon, J. Surprenant, Y. Tao, H. Xu, and L. A. Cuccia, Chem. Commun. 987 (2008).
[5] W. L. Noorduin, A. A. C. Bode, M. van der Meijden, H. Meekes, A. F. van Etteger, W. J. P. van Enckevort, P. C. M. Christianen, B. Kaptein, R. Kellogg, T. Rasing, and E. Vlieg, Nature Chem. **1**, 729 (2009).
[6] W. L. Noorduin, B. Kaptein, H. Meekes, W. J. P. van Enckevort, Richard M. Kellogg, and Elias Vlieg, Angew. Chem. Int. Ed. **48**, 4581 (2009).
[7] W. L. Noorduin, P. van der Asdonk, A. A. C. Bode, H. Meekes, W. J. P. van Enckevort, E. Vlieg, B. Kaptein, M. W. van der Meijden, R. M. Kellogg, and G. Deroover, Organic Process Res. Dev. **14**, 908 (2010).
[8] J. E. Hein, B. H. Cao, C. Viedma, R. M. Kellogg, and D. G. Blackmond, J. Am. Chem. Soc. **134**, 12629 (2012).

[9] L. Spix, A. Alfring, H. Meekes, W. J. P. van Enckevort, and E. Vlieg, Cryst. Growth Des. **14**, 1744 (2014).

[10] M. Iggland, M. P. Fernández-Ronco, R. Senn, J. Kluge, and M. Mazzotti, Chem. Eng. Sci. **111**, 106 (2014).

[11] R. R. E. Steendam, J. Dickhout, W. J. P. van Enckevort, H. Meekes, J. Raap, F. P. J. T. Rutjes, and E. Vlieg, Cryst. Growth Des. **15**, 1975 (2015).

[12] L.-C. Sögütoglu, R. R. E. Steendam, H. Meekes, E. Vlieg, and F. P. J. T. Rutjes, Chem. Soc. Rev. **44**, 6723 (2015).

[13] S. B. Tsogoeva, S. Wei, M. Freund, and M. Mauksch, Angew. Chem. Int. Ed. **48**, 590 (2009).

[14] M. Uwaha, J. Phys. Soc. Jpn. **73**, 2601 (2004).

[15] M. Uwaha, J. Phys. Soc. Jpn. **77**, 083802 (2008).

[16] J. M. McBride and J. C. Tully, Nature **452**, 161 (2008).

[17] M. Uwaha and H. Katsuno, J. Phys. Soc. Jpn. **78**, 023601 (2009); **79**, 068001 (2010) (errata).

[18] M. Uwaha, in *Selected Topics on Crystal Growth*, edited by M. Wang, K. Tsukamoto, and D. Wu, AIP Conf. Proc. No. 1270 (AIP, New York, 2010), p. 155.

[19] Y. Saito and H. Hyuga, J. Phys. Soc. Jpn. **73**, 33 (2004).

[20] Y. Saito and H. Hyuga, J. Phys. Soc. Jpn. **74**, 535 (2005).

[21] J. A. D. Wattis, Orig. Life Evol. Biosph. **41**, 133 (2011).

[22] M. Iggland and M. Mazzotti, Cryst. Growth Des. **11**, 4611 (2011).

[23] C. Blanco, J. Crusats, Z. El-Hachemi, A. Moyano, S. Veintemillas-Verdaguer, D. Hochberg, and J. M. Ribó, Chemphyschem. **14**, 3982 (2013).

[24] C. Blanco, J. M. Ribó, and D. Hochberg, Phys. Rev. E **91**, 022801 (2015).

[25] J. H. E. Cartwright, O. Piro, and I. Tuval, Phys. Rev. Lett. **98**, 165501 (2007); The mechanism of homochirality in this model is not identified, but likely to be the geometrical effect as pointed out in Y. Saito and H. Hyuga, Rev. Mod. Phys. **85**, 603 (2013).

[26] Y. Saito and H. Hyuga, J. Phys. Soc. Jpn. **79**, 083002 (2010).

[27] Y. Saito and H. Hyuga, J. Cryst. Growth **318**, 93 (2011).

[28] Y. Saito and H. Hyuga, J. Phys. Soc. Jpn. **77**, 113001 (2008).

[29] F. C. Frank, Biochem. Biophys. Acta **11**, 459 (1953).

[30] D. K. Kondepudi, R. Kaufman, and N. Singh, Science **250**, 975 (1990).

[31] For a review: D. K. Kondepudi and K. Asakura, Acc. Chem. Res. **34**, 946 (2001).

[32] V. Goldanskii and V. Kuzmin, Sov. Phys. Uspekhi **32**, 1 (1989).

[33] V. Avetisov and V. Goldanskii, Proc. Natl. Acad. Sci. USA **93**, 11435 (1996).

[34] W. L. Noorduin, H. Meekes, A. A. C. Bode, W. J. P. van Enckevort, B. Kaptein, R. M. Kellogg, and E. Vlieg, Cryst. Growth Des. **8**, 1675 (2008).

[35] H. Katsuno and M. Uwaha, J. Cryst. Growth **311**, 4265 (2009).

[36] F. Ricci, F. H. Stillinger, and P. G. Debenedetti, J. Chem. Phys. **139**, 174503 (2013).

[37] J. M. McBride, Lecture at NORDITA Workshop "Origins of homochirality" (2008), http://agenda.albanova.se/conferenceDisplay.py?confId=322.

[38] H. Katsuno and M. Uwaha, Phys. Rev. E **86**, 051608 (2012); J. Cryst. Growth **401**, 59 (2014).

[39] W. L. Noorduin, Willem J. P. van Enckevort, H. Meekes, B. Kaptein, R. M. Kellogg, J. C. Tully, J. M. McBride, and E. Vlieg, Angew. Chem. Int. Ed. **49**, 8435 (2010); C. Viedma, J. M. McBride, B. Kahr, and P. Cintas, *ibid.* **52**, 10545 (2013).

[40] Z. El-Hachemi, J. Crusats, J. M. Ribó, and S. Veintemillas-Verdaguer, Cryst. Growth Des. **9**, 4802 (2009).

[41] C. Viedma and P. Cintas, Chem. Commun. **47**, 12786 (2011).

[42] Change in temperature in vapor also amplifies EE: C. Viedma, W. L. Noorduin, J. E. Ortiz, T. de Torres, and P. Cintas, Chem. Commun. **47**, 671 (2011).

[43] K. Suwannasang, A. E. Flood, C. Rougeot, and G. Coquerel, Cryst. Growth Des. **13**, 3498 (2013).

[44] Gherase *et al.* [Cryst. Growth Des. **14**, 928 (2014)] proposed a model that modifies the population balance model of Iggland and Mazzotti [22] to reproduce the exponential amplification without agglomeration. Unfortunately, the modification mixed up the growth rate of the crystal radius and the total mass in Eq. (6) of the paper, which introduced an unphysical nonlinear effect. The Monte Carlo cluster model of Ref. [34] shows an exponential amplification, which is probably due to an improper choice of time increment (a decrease in the cluster number increases the apparent growth rate).

[45] M. Uwaha, J. Cryst. Growth **318**, 89 (2011).

[46] M. Iggland, R. Müller, and M. Mazzotti, Cryst. Growth Des. **14**, 2488 (2014).

[47] O. Penrose, J. Stat. Phys. **89**, 305 (1997).

[48] M. Uwaha and K. Koyama, J. Cryst. Growth **312**, 1046 (2010).

[49] For representing right and left species (enantiomers), *d* (dextrorotatory) and *l* (levorotatory) are used according to rotation of polarization of light passing through the material. D and L are typically used in biophysical literature, say, with respect to chirality of DNA, RNA, amino acids, and sugars according to stereochemical structure, which is usually connected to *d* and *l*. In chemical literature, *R* and *S*, representing rectus and sinister, are used according to stereochemical structure. In the present paper we simply use R and L.

[50] K. Suwannasang, G. Coquerei, C. Rougeot, and A. E. Flood, Chem. Eng. Technol. **37**, 1329 (2014).